

RESEARCH ARTICLE

Laser spectroscopy: A potential versatile solution for radiocarbon analyses

Zuguang Guan¹ , Yan Zhou¹, Qiang Ling¹, Luca Varricchio^{2,4}, Amelia Detti³, Saverio Bartalini^{2,3} and Daru Chen¹

¹Centre for Environmental and Climate-Change Research, Zhejiang Normal University, 311231 Hangzhou, China, ²CNR-INO and LENS, Via Carrara 1, 50019 Sesto Fiorentino, FI, Italy, ³ppqSense s.r.l., Viale Ariosto 492/B, 50019 Sesto Fiorentino, FI, Italy and ⁴University of Pisa, Department of Pharmacy, Via Bonanno 6, 56126 Pisa, Italy

Corresponding author: Zuguang Guan; Email: zgguan@zjnu.edu.cn

Received: 31 October 2024; **Revised:** 26 January 2025; **Accepted:** 07 February 2025; **First published online:** 13 March 2025

Keywords: applications; laser spectroscopy; radiocarbon; sample preparation; Saturated absorption Cavity Ring-down spectroscopy (SCAR)

Abstract

Radiocarbon (¹⁴C) measurements play important roles in dating and tracing applications where the isotopic concentration can differ from 0.1 to 10⁶ pMC (percent modern carbon). A liquid scintillation counter cannot provide enough sensitivity when dealing with low-concentration samples of limited amounts over a reasonable time period. Accelerator mass spectroscopy (AMS) measures low-concentrations well but must first do dilution for high-concentration samples, and suffers from high instrument and maintenance costs. Saturated absorption Cavity Ring-down spectroscopy (SCAR) has now been developed into a practical technique with performances close to AMS but at much lower costs. The dynamic range covers 1–10⁵ pMC, and the measurement uncertainties in the range of 0.4–1 pMC can be achieved within 0.5–2.5 hr of operation time. SCAR measures CO₂ gases directly without graphitization in sample preparation. The typical sample consumption is ~1 mg of carbon mass and the time for sample preparation can be as short as 15 min. Applications of SCAR to Suess-effect evaluation, biogenic-component analysis, ancient- and modern-sample dating, food-fraud detection and medicine-metabolism study have all been demonstrated by employing a close-to-automatic sample preparation system.

1. Introduction

In 1940s, scientists discovered the production of a rare carbon isotope (¹⁴C, approximately one in 10¹² parts of ¹²C) in the atmosphere (Korff and Danforth 1939; Korff et al. 1940) and its participation in the global carbon cycle through photosynthesis and food chain. Willard Libby and his group observed the absence of ¹⁴C in fossils and revealed its declining presence due to radioactive decay (Libby et al. 1970). Radiocarbon has since then presented importance in versatile applications (Hajdas et al. 2009), ranging from dating ancient (in e.g. Quaternary study and archaeology) or modern (in e.g. forensic science) samples, tracing metabolic pathways in human bodies, to determination of bio-/fossil- components (in fuel, fabric, or even the emissions of green-house gases and particulate pollution) for environmental considerations.

In different applications, samples under test may contain a wide dynamic range of the isotope. Figure 1 presents an exponential distribution of pMC (percent modern carbon) in the x-axis. One modern carbon (MC) is defined as the radioactivity of ¹⁴C in the atmospheric background in 1950, the year 0 BP (before present) in dating. In the earth science and archaeological studies, the limit of the ¹⁴C

© The Author(s), 2025. Published by Cambridge University Press on behalf of University of Arizona. This is an Open Access article, distributed under the terms of the Creative Commons Attribution-NonCommercial-ShareAlike licence (<https://creativecommons.org/licenses/by-nc-sa/4.0/>), which permits non-commercial re-use, distribution, and reproduction in any medium, provided the same Creative Commons licence is used to distribute the re-used or adapted article and the original article is properly cited. The written permission of Cambridge University Press must be obtained prior to any commercial use.

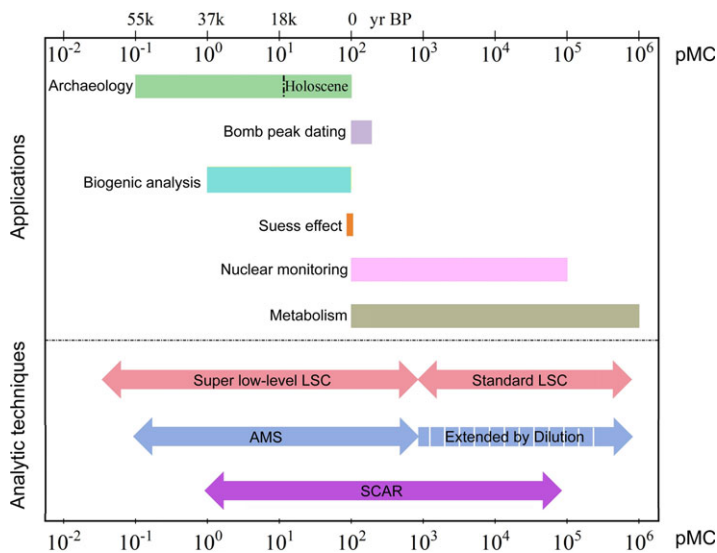


Figure 1. The dynamic ranges of the radiocarbon's contents in different types of samples and their coverage by different analytic techniques.

dating method is around 55 kyr BP (Hajdas et al. 2021), when the radioactivity of such an ancient sample decays into 0.1 pMC. For modern samples after 1950, ^{14}C contents present a sharp increase to ~ 200 pMC in 1960s and decrease back to < 100 pMC at present (Hua et al. 2022; Kutschera 2022). The atmospheric nuclear tests were restricted after 1960s, and the abnormal abundance was absorbed by oceans and terrestrial systems and also diluted by fossil emissions. The so-called bomb-peak curve is employed for dating modern samples in e.g. forensic investigations (Hajdas et al. 2022; Johnstone et al. 2023; Kutschera 2022; Quarta et al. 2019; Wang et al. 2010; Zavattaro et al. 2007). Because of the increasing awareness of environmental protection and sustainable economy, the utility of fossil-based materials is now limited and replaced more and more by the use of recyclables. ^{14}C therefore becomes a remarkable tracer to distinguish fossil and biogenic materials in e.g. fuels, fabrics, plastics, leathers, etc. (Carcione et al. 2023; Delli et al. 2021; Varga et al. 2023; Wang et al. 2022). In 1949, Suess discovered that the ^{14}C content in the atmosphere decreases because of the dilution by the CO_2 emission from the fossil combustion (Suess et al. 1955). ^{14}C is considered the most promising tracer for evaluating the anthropogenic CO_2 emission, which is a major factor responsible for global climate change (Cui et al. 2019; Michael et al. 2012; Pataki et al. 2010; Turnbull et al. 2007; Zhou et al. 2022). Such a dilution effect (Suess-effect) is usually not large, e.g., the anomalies in the downtown of a mega-city is only ~ 10 pMC below the background value (Pataki et al. 2010). Measurement resolution below 0.1 pMC is required for Suess-effect evaluation, and this is quite challenging to analytical methods. Leakage risks of nuclear power plants, on the other hand, are another environmental concern. The finding of abnormally increased concentrations (up to several hundred times of MC) in the surrounding atmosphere and hydrosphere, or in biosphere over accumulation, can help to reveal and evaluate such risks (Buzynnyi et al. 2023; Cao et al. 2024; Krishnan et al. 2022). ^{14}C is also a perfect candidate to trace the medicine metabolic pathways and the micro-dosing technique has shown significant advantages for studies directly on human bodies for many obvious reasons (Arjomand et al. 2010; Gao et al. 2011; Zoppi et al. 2007; Zoppi et al. 2010). The safety limit for human beings is 250 nCi (Arjomand et al. 2010). However, such a level of ^{14}C in a human body is still hundreds even thousands of times above the atmospheric background.

The development of ^{14}C analytical methods has been driven by the needs in these applications. Libby's brilliant screen-wall counter plotted the famous "curve of knowns" and deduced the half-life of ^{14}C (Arnold et al. 1949) but was soon replaced by proportional gas counters (Vries and Barendsen 1953)

and later by liquid scintillation counters with much higher detection efficiency (Nazarov et al. 2021). By applying massive lead shielding and coincidence counting techniques, ultra-low background (0.038 pMC) can be achieved using modern super low-level LSCs, which are ideal for very old samples (Hogg et al. 2022). LSCs dominated in archaeology and Quaternary study until the rise of accelerator mass spectroscopy (AMS) in 1970s. The latter has revolutionary advantages in the reduction of sample sizes and time consumption. However, up to date, LSCs are still frequently used in nuclear monitoring and medicine metabolism research, where sample consumption is not a problem and the higher radioactive levels in samples make the measurement time acceptable (Buzynnyi et al. 2023; Cao et al. 2024; Krishnan et al. 2022; Zollinger et al. 2014). After 40 years of development, AMS has become the king of ^{14}C analysis. Sample size down to 10 μgC and precision of 1‰ using 1 mgC within 1 hr of measurement are realized by a compact AMS with footprint size of $\sim 8\text{ m}^2$ (Synal et al. 2007). AMS is an extremely sensitive instrument with a detection limit $< 0.1\text{ pMC}$, but its dynamic range is usually within 10^4 , which is not sufficient for metabolism applications. Therefore 100- to 1000-fold dilution is needed when AMS is employed for medicine samples (Arjomand et al. 2010). These systems are not recommended to be shared with low-level measurements for the background contamination reason. Moreover, the acquisition and operation of an AMS instrument still have to bear a relative high cost. Laser spectroscopy (LS) on radiocarbon measurements has attracted enormous efforts (Fatima et al. 2021; Giusfredi et al. 2010; Galli et al. 2016; Jiang et al. 2021; McCart et al. 2016; Zare et al. 2012) and one of the most successful techniques is called Saturated-absorption Cavity Ring-down spectroscopy (SCAR) (Giusfredi et al. 2010). Through the continued improvement over the last decade, SCAR has now been commercialized at the ppqSense company, with performances quite close to AMS but with a much less cost. The lower detection limit is 1 pMC and the upper limit is 10^5 pMC . A precision of 0.3 pMC can be achieved by averaging the absorption signal in 4 hr. Laser spectroscopy method offers new opportunities for applications where AMS is deemed too complicated and expensive, meanwhile LSC is inappropriate for sample processing complexity and time consumption reasons.

In this paper, the working principle of SCAR and its sample preparation procedure are described. Samples in different phases were prepared and measured to demonstrate the feasibilities of the technique in different applications including Suess-effect evaluation, biogenic component analysis, food fraud detection, dating, and medicine metabolism study. In the final section, the performances of the SCAR technique are concluded and discussed.

2. Methodology

2.1 Saturated absorption Cavity Ring-down spectroscopy (SCAR)

SCAR is a special Cavity Ring-Down laser Spectroscopy (CRDS) by employing the saturated absorption region of the ring-down curve to reduce noises induced by the mechanical vibration and therefore increase the sensitivity dramatically. The working principle of the technique has been described in detail in (Giusfredi et al. 2010; Galli et al. 2016; Zare et al. 2012).

As a molecular absorption spectroscopy, SCAR measures $^{14}\text{CO}_2$ concentration in pure CO_2 gas sample by scanning the laser wavelength through 2208–2212 cm^{-1} to cover the absorption line (0001-0000) P(20) of $^{14}\text{CO}_2$ molecule and fitting the absorption spectrum with a Voigt function. As shown in Figure 2(a), the spectral area covered by the fitting curve is proportional to the abundance of the molecule, and the fitting residual is used to evaluate the measurement uncertainty. It is possible to derive the systematic error using multiple measurements of the same sample. To report the measurement result in percent Modern Carbon (pMC) or Fraction Modern ($F^{14}\text{C}$), the $^{14}\text{CO}_2$ abundance needs to be calibrated by reference materials and corrected by the fractionation factor of isotope ^{13}C (i.e. $\delta^{13}\text{C}$) (Stuiver and Polach 1977). $\delta^{13}\text{C}$ values of CO_2 gases can be either measured by an Isotope Ratio Mass Spectroscopy (IRMS), a Cavity Ring-Down Spectroscopy (CRDS), or obtained through looking up empirical data (Julien et al. 2015). Figure 2(b) shows a standard 4-point accuracy analysis on reference materials IAEA C1, C7, C8, and NIST OXII, and a root-mean-square deviation of 0.50 pMC is

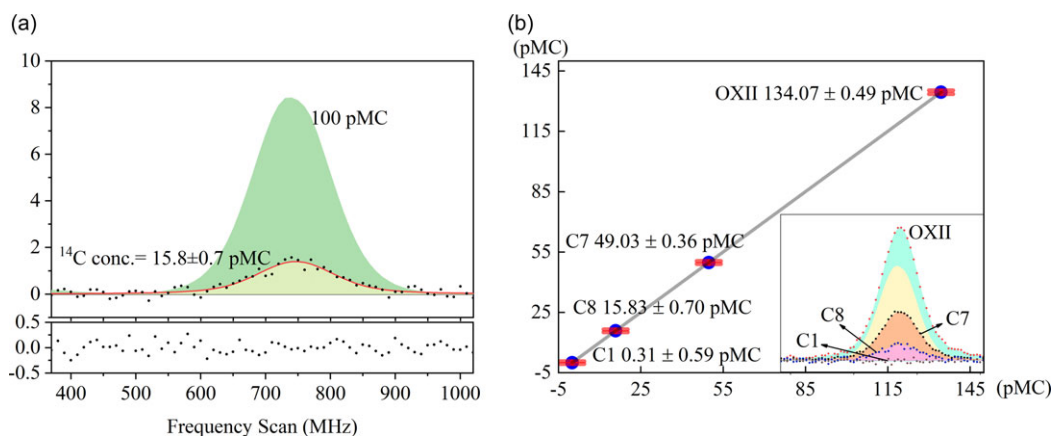


Figure 2. (a) The spectral area (the yellow green) below the fitting curve (red) is proportional to the ^{14}C abundance. The green spectral area (100 pMC) is plotted for comparison. The fitting residuals in the bottom is to calculate the uncertainty of the result. (b) Reference materials IAEA C1, C7, C8 and NIST OXII are used to evaluate the absolute accuracy of the technique by calculating the root-mean-square deviation.

achieved. A 2-point calibration has been performed by using IAEA C1 as 0 pMC point and the NIST OXII standard as 134.07 pMC point. $\delta^{13}\text{C}$ values of the reference materials are from suppliers and have been applied in the above calibration and data-quality assurance.

It is worthwhile mentioning that to avoid the interference from the N_2O molecules which have absorption line located very close to the chosen $^{14}\text{CO}_2$ line, the absorption cavity is stabilized at the low temperature (170 K) and low pressure (12 mbar) to keep the spectral profile sufficiently narrow. The N_2O gas is expected to be well removed in the sample preparation procedure (described below). For some cases where residual N_2O does induce interference (which can be observed in the absorption spectrum), an extra fitting algorithm on the N_2O spectrum will be applied to compensate the measurement.

2.2 Sample preparation for SCAR

SCAR is designed to measure $^{14}\text{CO}_2$ in pure CO_2 gas. With a preparation system, it is able to measure solid, liquid and gaseous samples containing radiocarbon. The procedure is similar to the established technique (Aerts-Bijma et al. 2001). The flow chart of sample preparation is shown in Figure 3. Solid samples are cut into small pieces and weighted by a high precision digital analytic balance, while liquid samples are picked and measured by a micro-pipette. They are packaged by Tin cups and combusted at an elemental analyzer (ESC 8020 CHNS/O, NC Technologies S.R.L.) into CO_2 gases. The elemental analyzer is a furnace (operated in 950°C) connected with gas filters and a gas chromatography (GC) to separate CO_2 from other gases. The gaseous sample, ambient air, is prepared by a gas concentrator (ESC 8070 Air CO_2 , NC Technologies S.R.L.) where CO_2 in the air sample is purified and accumulated. The CO_2 gas is delivered from ESC 8020 or ESC 8070 by a helium carrier gas to a homemade zeolite filter or a glass flask bathed in liquid nitrogen, where the helium gas passes through and the CO_2 gas is trapped. The zeolite filter is connected to SCAR cavity and CO_2 is released into it automatically by heating the zeolite. The glass flask connects to SCAR manually for flexibility in applications.

To fill the absorption cavity sufficiently, a minimum carbon mass ~ 1 mg is required. The typical time for ESC 8070 or ESC 8020 to prepare such amount of CO_2 is ~ 15 min. The measurement time of SCAR ranges from minutes to hours for different uncertainty levels on-demand.

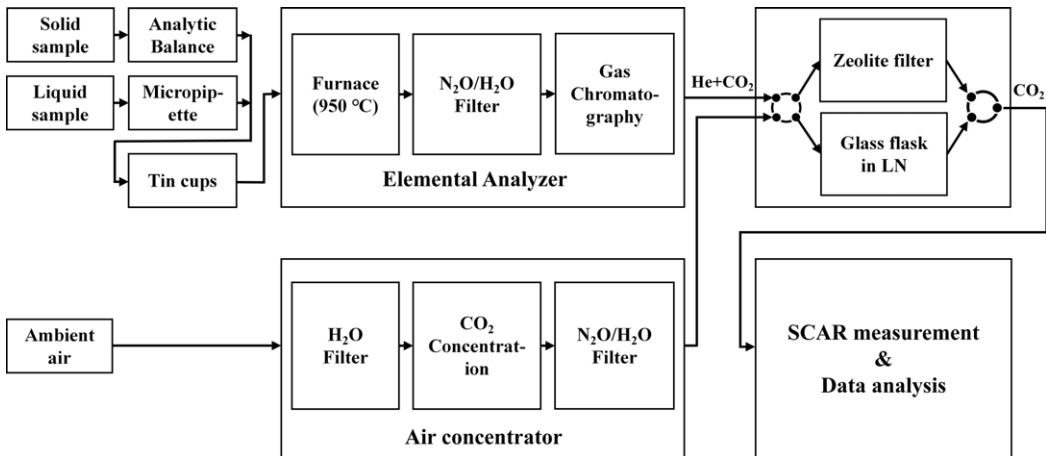


Figure 3. The flow chart of the sample preparation for SCAR.

Water vapor and N_2O gas are harmful to the measurement. The former will be frozen on the high-reflectivity mirrors at the low temperature in the cavity, and the latter is an interference gas as aforementioned. Specific filters are thus designed in ESC 8070 and ESC 8020 to remove them. Water vapor is absorbed by SICAPENT[®] trap, and the N_2O is removed by a copper-powder column heated to 550°C .

3. Measurements and results

3.1 Suess effect evaluation

To observe the Suess effect induced by the fossil emission, the same kind of plants (*Bromus*) were collected from two different locations at a town close to the city of Florence in Italy. Some samples are from a rural area, and the others are from the roadside close to a gas station where the traffic is quite busy. The plants were already dry when collected, and they were prepared in laboratory by weighting and packaging before being combusted in the elemental analyzer. The carbon-content ratios were measured to be around 30%, and ~ 5 mg of raw leaves was sufficient for SCAR to analyze its ^{14}C abundance.

The ambient air of an industrial area (outside the Florence city where the laboratory of ppqSense company locates) was collected and CO_2 in the air sample was concentrated by ESC 8070. The enrichment time was 15 min and totally 16.5 mg of CO_2 (i.e. 4.5 mg carbon mass) was collected. The measurement procedure takes from 30 min to hours, depending on the measurement accuracy. In this experiment, a measurement uncertainty of ± 0.5 pMC was achieved in 90 min of averaging. A quasi-continuing measurement with time resolution of 30 min can be expected, which is a solid competitive advantage over AMS and LSC for the ambient air monitoring.

In Figure 4, the measurement results are presented in $\Delta^{14}\text{C}$, indicating the deviation of ^{14}C in parts per thousand (per mil) from the preindustrial atmosphere (Reimer et al. 2004). To do fractionation corrections, the $\delta^{13}\text{C}$ values of the ambient air ($-9 \pm 3\text{‰}$) and of the plants ($-28.10 \pm 2.5\text{‰}$) are obtained from literatures (Stuiver and Polach 1977; Troughton and Card 1975). $\Delta^{14}\text{C}$ value of the background atmosphere in 2024, which works as the reference, is deduced by applying an annual decrease of 5‰ on the 2019 data (Hua et al. 2022). The local ambient air (of the industrial area) and the plants from the roadside present clear decreases, while the plants collected in the rural region does not. This reveals that the atmospheric $^{14}\text{CO}_2$ in the industrial area and at the road side are diluted by the emissions from fossil fuels.

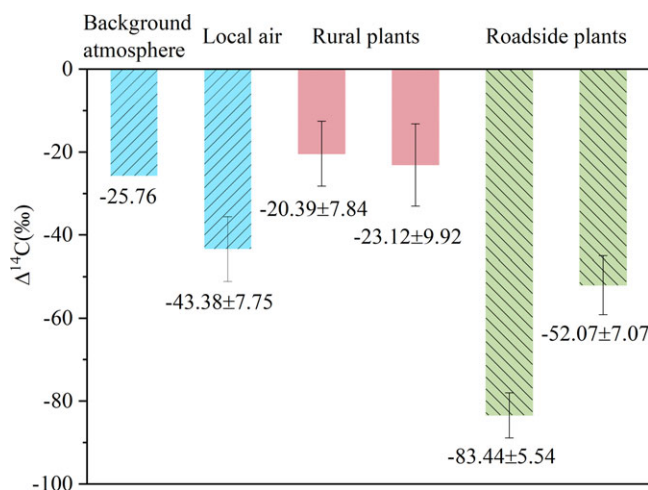


Figure 4. The air from the local industrial area and the plants from the roadside contain less ^{14}C while the rural plants present an equivalent level, comparing with the background atmosphere.

3.2 Biogenic content analysis

As global warming and climate changes progressively increases social concerns, the restriction on fuels and raw materials from fossils has become a common awareness to reduce CO_2 emissions. Adding biogenic content into fossil fuels such as petrol, nature gas and coal is an effective practice and has become national policies in many countries, and the application of fossil-limited/free materials in fashion market becomes a trend. Radiocarbon measurement provides scientific backing in determining the biogenic content in fuels or fashion materials. SCAR has been proven to be a novel and effective technique for such applications. It was applied to analyze biogenic components in fuels (Delli et al. 2021) and fashion materials (Carcione et al. 2023), and the results were consistent with AMS.

In this paper, two bio-plastic materials were analyzed by SCAR. Plastic-1 is from a disposable cutlery case containing a PLA (polylactic acid) material. Plastic-2 is from a supermarket (Coop Italy) shopping bag containing a registered bio-plastic material called Mater Bi[®]. For the two materials, 6 mg and 5.4 mg samples were prepared and measured, respectively. Both materials contain a similar carbon-mass content ($\sim 40\%$) but different radiocarbon abundances (14.64 ± 0.88 and 66.22 ± 0.88). Although no fractionation correction is performed, distinct values (15% and 66%) of the bio-mass ratios for the two materials are still well deduced, respectively, by assuming the radiocarbon abundance of pure bio-materials to be one hundred percent Modern.

3.3 Dating

To demonstrate the feasibility of SCAR for dating applications, ancient and modern (after 1950) samples were respectively analyzed. Modern samples include a bottle of white wine in 1979, and a piece of wood collected from an old gate in the downtown of Florence. The exact age of the gate is not known. The ancient sample is 950 mg of a sediment from Chinese Academy of Geological Sciences (CAGS). The sediment was pretreated with the acid-base-acid (ABA) method and the ^{14}C and ^{13}C abundances were measured by AMS at CAGS. The zero-background graphite used at the AMS is also measured by SCAR for comparison.

0.05 mL of the white wine and 8.8 mg of the gate wood were used in the measurements. The ^{14}C abundances of the wine and the wood were measured, and the values of Fraction Modern ($F^{14}\text{C}$) were deduced to be 1.2934 ± 0.0088 and 1.0726 ± 0.0126 , respectively. $\delta^{13}\text{C}$ of the two samples were from

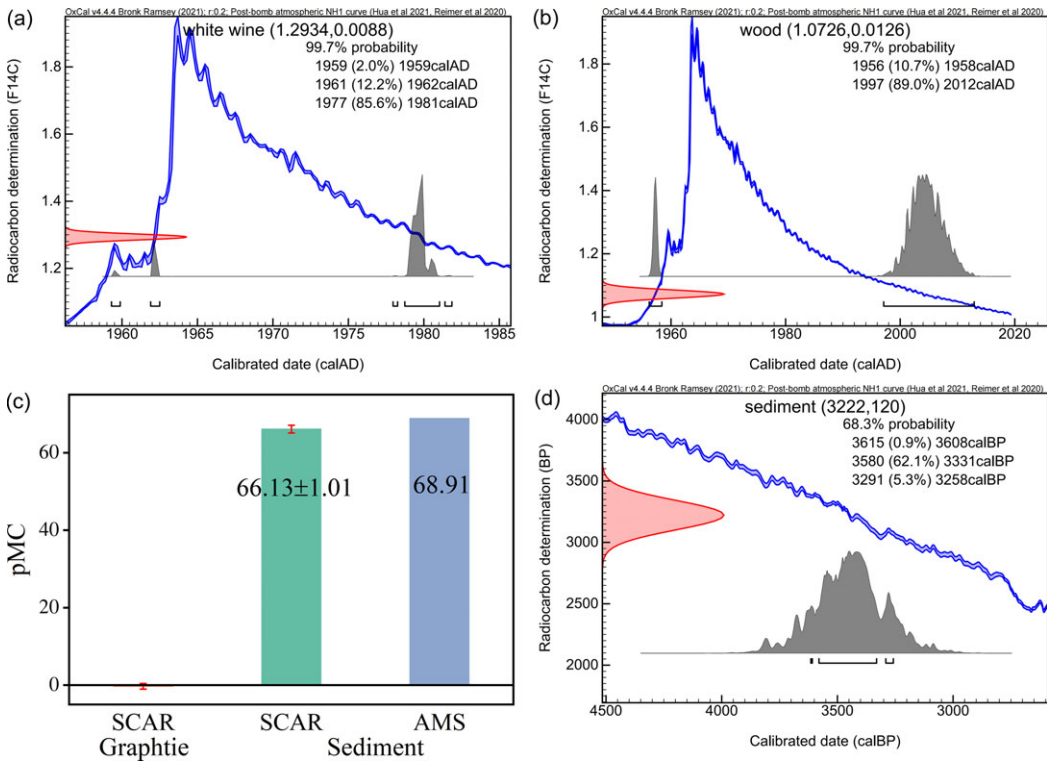


Figure 5. Dating the ages of the white wine (a) and old wood (b) samples with bomb-peak curve. The comparison of the results between the SCAR and AMS measurements (c) and the age evaluation (d) of the sediment. The measurement on the background graphite in (c) is for the zero-point check.

literatures (Stuiver and Polach 1977; Troughton and Card 1975), i.e. $-28.10 \pm 2.5\%$ and $-25 \pm 5\%$ for grape and wood, respectively. Applying the bomb-peak curve, the age of the white wine is determined to be 1979 ± 2 calendar year (Figure 5(a)). For the wood, Figure 5(b) indicates two possibilities, and we believe the real age of the tree is more likely in 1956–1958, since the appearance of the old gate suggests that the tree should not have been cut down later than 2000.

Since the carbon content of the sediment was measured to be only $\sim 0.2\%$, to accumulate enough CO_2 for measurement, 950 mg of sediment was divided equally into 10 parts (i.e. 100 mg/part and the last being 50 mg) and combusted using the EA individually. The CO_2 was collected by the glass flask bathed in liquid nitrogen. The accumulated CO_2 was finally fed into SCAR for measurement. The measured ^{14}C abundance of the sediment was 67.10 ± 1.01 before doing $\delta^{13}\text{C}$ correction. The interference from N_2O gas appeared in the measurement and the compensation algorithm was applied. An abnormally high uncertainty ± 1.01 was produced even we had averaged the signal for 90 min. The fractionation factor $\delta^{13}\text{C}$ (-24.08%) obtained from the AMS measurement at CAGS was employed for correction, although this value differs from that of the original CO_2 gas before graphitization (Fahrni et al. 2017). After $\delta^{13}\text{C}$ correction, our result is 66.96 ± 1.01 , which is consistent with the AMS result of 68.91 pMC, see Figure 5(c). The age of the sediment is determined to be 3222 ± 120 yr BP (Figure 5(d)).

3.4 Food fraud detection

Radiocarbon was utilized to detect food fraud (Palstra et al. 2024; Quarta et al. 2022; Tudyka et al. 2014; Varga et al. 2023) by analyzing the biological component or determining the age of the food and

Table 1. Measurement results and evidence to answer questions regarding food fraud detection

Sample	pMC (with $\delta^{13}\text{C}$ correction)	$\delta^{13}\text{C}$	Bio-carbon ratio	Age	Question	Answer
White wine	129.34 ± 0.88	$-28.10 \pm 2.5\text{‰}$	—	1979 ± 2	Is the wine from 1979?	Yes
White vinegar	98.45 ± 1.32	$-23 \pm 5\text{‰}$	$\sim 98\%$	—	Is the vinegar from fermentation?	Yes
Cake cream	98.04 ± 1.18	$-20 \pm 4\text{‰}$	—	2024 ± 2	Is the cream made of old gelatin?	No
Guiling jelly	97.90 ± 1.12	$-20 \pm 4\text{‰}$	—	2024 ± 2	Is the jelly made of old gelatin?	No

beverage. For instance, vinegar in many countries is obliged to be produced from plants through the fermentation process while acetic acid is also available by industrial synthesis from fossil materials. The latter has a lower cost and hence is possibly used to produce synthetic vinegar. In China, the national standard (GB1886.10-2015) states that the ratio of the natural (biological) component in vinegar should be above 95%. Aged wines and liquors are usually of higher quality, so the fraudulent production of aged and expensive alcohols is often mixed with younger ones. Radiocarbon abundance in the ethanol reveals the real age of the alcohol, i.e., the exact year the grape or wheat was planted. Different from acetic acid, gelatins are from nature proteins, whether as food additive or for industrial usage. Edible gelatin is from fresh materials and usually with a shelf-life less than 2 years. Industrial gelatin, however, is possible to come from recycled materials and thus might have older radiocarbon age. It was reported that industrial gelatin was illegally used as a food additive for cost saving.

To verify the performance of SCAR in such applications, a bottle of white wine from 1979, a bottle of white vinegar (made in 2024), some cream in a packaged Macaron cake and some Chinese Guiling jelly (the latter two contain gelatin) were tested. 0.05 mL of wine, 0.15 mL of vinegar, 5.9 mg of cake cream, and 50 mg of jelly were prepared and measured. No special treatment was applied before the combustion and the measurement procedure that takes 30 or 60 min/sample.

Table 1 shows the measurement results and evidences to support the use of SCAR for food fraud detection. The values of $\delta^{13}\text{C}$ are from literatures (Stuiver and Polach 1977; Troughton and Card 1975). Dating with the bomb-peak curve (see Figure 5(a)), the age of the white wine is determined to be 1979 ± 2 . The bio-carbon ratio in the vinegar is higher than 95% (the Chinese national standard for fermented vinegar) by assuming the ^{14}C abundance of pure bio-materials to be 100 pMC. The carbon in both cake cream and jelly are proven to be from young materials and there is no old gelatin added.

3.5 Medicine metabolism study

To test the performance of SCAR to its upper detection limit, human metabolic samples labeled with ^{14}C were analyzed. Three plasma samples, two urine samples, and one feces sample were prepared and measured. The sources of the samples are not revealed for confidential reasons.

Among the three plasma samples, two (Plasma-2 and Plasma-3) are from experimental groups who took the ^{14}C -labeled medicine while sample Plasma-1 is from the control group who did not take the medicine. 0.1 mL (100 mg) of each sample were combusted by EA directly and measured by SCAR. The measurement times for the three samples are 30, 10, and 2 min respectively. From Figure 6, one can see that Plasma-1 from the control group, presents 99.03 pMC close to the nature background, while the other two samples present around 8.6 and 38 times of the background, respectively. Similar to the plasma samples, the sample Urine-2 is from the experimental group and Urine-1 is from the control group. The urine was absorbed on a piece of paper and the paper was dried and cut into small pieces

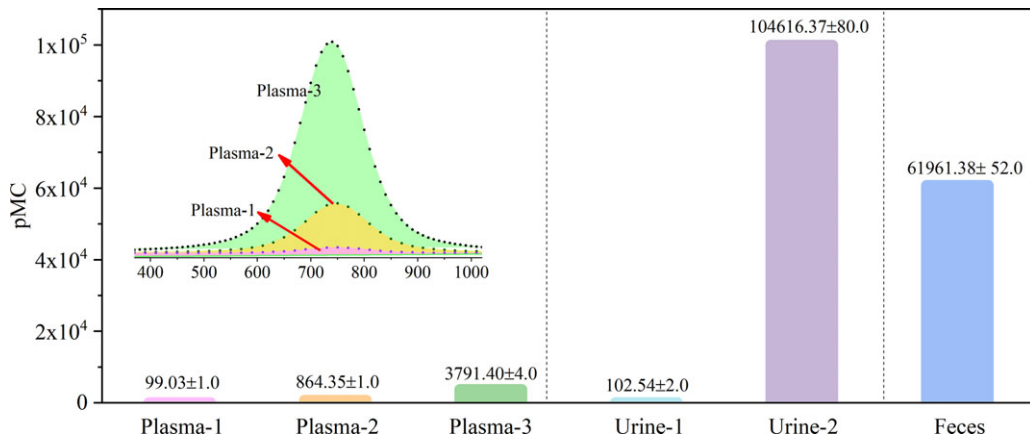


Figure 6. The comparison between experimental and control groups among different metabolic samples (left: plasma; middle: urine; right: feces). The inset shows the spectral areas of different plasma samples.

(~30 mg) for combustion and measurement. The carbon masses of the urine samples on the papers were, however, not measured. The ^{14}C concentration of the experimental group is beyond 10^5 pMC, 1000 times of that measured in the control group. The real concentration of the urine is believed to be even higher since it has been diluted by the carbon mass of the paper. The feces sample is only from the experimental group and there is no control group for reference. 33 mg of sample was directly combusted and measured, and $\sim 6 \times 10^4$ pMC of ^{14}C was observed.

4. Conclusion and discussion

In conclusion, a total of 24 (16 solid, 7 liquid and 1 gaseous) samples were prepared and analyzed using SCAR, in the laboratory at the ppqSense company in Florence. The time consumption, the sample mass, and the measurement results (with and without $\delta^{13}\text{C}$ correction) of each sample are listed in Table 2.

From the table, one can see that the minimum carbon mass measured using SCAR is 1.4 mg. According to the ppqSense company, the minimum value is now 0.6 mg for the newest version of SCAR. This is competitive with LSC but still worse than AMS. To obtain this amount of carbon mass, in most cases, we need several to tens of mg in raw materials. They can be combusted using an EA in one working cycle since the maximum sample mass taken by the EA is suggested to be <100 mg. It is an exception for the white vinegar and the sediment, in which the carbon mass ratio is very low (1.3% and 0.2% respectively). 150 mg of vinegar and 950 mg of sediment were utilized, and they were separated into equal parts and combusted for 2 and 10 times, respectively. For the ambient air, in a 15-min cycle by the ESC 8070, a total of 21 L air was concentrated and 16.5 mg CO_2 was trapped at the zeolite filter.

The sample-preparation and measurement procedures for SCAR are relatively simple. Unlike AMS where graphitization is required and LSC where the scintillation liquid needs to be prepared, SCAR analyzes CO_2 gases directly. The samples can be combusted directly by EA and the CO_2 gas can be trapped by the zeolite filter. The entire preparation procedure is automatic and takes only 15 min. Even in the most difficult case with sediment, where the sample is divided and combusted for 10 times, the preparation time (105 min) is acceptable. The SCAR measurement is also automatic, and the time taken for one sample ranges from 30 min to hours, depending on the uncertainty required by the applications (discussed later). For high-concentration samples like in medicine metabolism studies, the measurement time can be reduced to several minutes. The preparation and measurement procedures are independent

Table 2. The summary of 24 samples prepared and analyzed by SCAR measurements

Application	Sample state	Sample name	Sample source	Preparation time (min)	Measurement time (min)	Raw mass (mg)	C-mass(mg) / ratio	¹⁴ C abundance (without δ ¹³ C correction)	δ ¹³ C (‰)	pMC (with δ ¹³ C correction)
Quality assurance	Solid	C1	IAEA	15	60	25	3 (12%)	0.3 ± 0.59	-2.24	0.31 ± 0.59
	Solid	C7	IAEA	15	150	13.5	2.2 (16%)	50.09 ± 0.36	-14.48	49.03 ± 0.36
	Solid	C8	IAEA	15	30	11.2	1.8 (16%)	16.05 ± 0.70	-18.30	15.83 ± 0.70
	Solid	OX-II	NIST	15	90	14	2.5 (18%)	136.05 ± 0.49	-17.80	134.07 ± 0.49
Suess-effect evaluation	Gas	Ambient air	Sesto Fiorentino	15	90	16.5	4.5 (27.3%)	99.72 ± 0.51	-9 ± 3	96.35 ± 0.78
	Solid	Leaf-1	Road side	15	60	4.85	1.5 (31.7%)	91.89 ± 0.55	-28.10 ± 2.5	92.48 ± 0.73
	Solid	Leaf-2	Road side	15	90	6.48	2.1 (32.1%)	95.04 ± 0.51	-28.10 ± 2.5	95.65 ± 0.71
	Solid	Leaf-3	Rural	15	60	4.34	1.4 (31.8%)	98.21 ± 0.60	-28.10 ± 2.5	98.85 ± 0.79
	Solid	Leaf-4	Rural	15	30	6.77	2.1 (30.4%)	97.94 ± 0.89	-28.10 ± 2.5	98.57 ± 1.03
Biogenic analysis	Solid	Plastic-1	Disposable cutlery case, PLA	15	30	6	2.5 (41%)	14.64 ± 0.88	—	—
	Solid	Plastic-2	Shopping bag, MaterBi®	15	30	5.4	2.2 (40%)	66.22 ± 0.88	—	—
Dating	Solid	Graphite	CAGS	15	30	2.8	2.0 (72%)	-0.28 ± 0.72	—	—
	Solid	Sediment	CAGS	105	90	950	1.9 (0.2%)	67.10 ± 1.01	-24	66.96 ± 1.01
	Solid	Wood	Downtown in Florence	15	60	8.8	3.1 (35%)	107.25 ± 0.59	-25 ± 5	107.26 ± 1.26
Food-fraud detection	Liquid	White wine	Villa antinori 1979	15	60	50	2.0 (4%)	128.51 ± 0.57	-28.10 ± 2.5	129.34 ± 0.88
	Liquid	White wine	Villa antinori 1979	15	60	50	2.0 (4%)	128.51 ± 0.57	-28.10 ± 2.5	129.34 ± 0.88
	Liquid	White vinegar	Zhenjiang, China	25	60	150	2.0 (1.3%)	98.85 ± 0.83	-23 ± 5	98.45 ± 1.32
	Solid	Cake cream	Orion Pie (China)	15	30	11	2.8 (25%)	99.05 ± 0.85	-20 ± 4	98.04 ± 1.18
	Solid	Jelly	Guiling Jelly (China)	15	30	50	2.0 (4%)	98.90 ± 0.77	-20 ± 4	97.90 ± 1.12
Metabolism	Liquid	Plasma-1	Unknown	15	30	100	4.0 (4%)	99.03 ± 1.0	—	—
	Liquid	Plasma-2	Unknown	15	10	100	4.0 (4%)	864.35 ± 1.0	—	—
	Liquid	Plasma-3	Unknown	15	2	100	4.0 (4%)	3791.40 ± 4.0	—	—
	Liquid	Urine-1	Unknown	15	—	30	8.4 (28%)	102.54 ± 2.0	—	—
	Liquid	Urine-2	Unknown	15	—	30	9.9 (33%)	104616.37 ± 80	—	—
	Solid	Feces	Unknown	15	—	33	15.5 (47%)	61961.38 ± 52	—	—

and thus can be operated in parallel: when a delivered CO₂ gas sample is under measurement, a new cycle of combustion or enrichment can start at ESC 8020 or ESC 8070. These advantages make SCAR a potential candidate in commercializing integrated radiocarbon laboratories, which is very difficult for AMS or LSC techniques to realize. It is worthwhile to mention that SCAR is probably the only technique hopeful in realizing real-time (or near real-time) ambient radiocarbon measurement in the future. This would be especially valuable to e.g. the fossil-emission evaluation and source identification, the nuclear leakage monitoring, etc.

SCAR's measurement range is broad, with the lower limit of detection (LLD) to 1 pMC and the upper limit to 10⁵ pMC. AMS performs better near the LLD (<0.1 pMC) region, but its dynamic range is usually limited to 10⁴. LSC theoretically can measure low concentration, but the sample and time consumptions are not so practical when ¹⁴C abundance is close to or below the natural background. The broad measurement range of SCAR makes it a versatile solution for many applications. For archaeological studies, the theoretical age limit is 37 kya (corresponding to the LLD 1 pMC). However, in practice the measurement uncertainty at such a low concentration cannot support the dating precision. 18 kya (corresponding to 10 pMC) is realistic and can cover Holocene in earth science research. SCAR provides promising measurements in the range of several to hundreds of pMC, which covers applications such as biogenic-component analysis, dating with the bomb-peak curve, and Suess-effect evaluation. Due to its broad dynamic range, SCAR can measure up to 1000 times above the natural background and therefore is able to quantify the ¹⁴C tracers in human plasma, urine, and feces directly without applying the dilution process.

The uncertainty can be reduced as the measurement time increases. From Table 2, one can see that the uncertainties within ±1, ±0.6, and ±0.4 pMC can be achieved by increasing the measurement time from 30 min, to 1 h and 2.5 hr, respectively. For biogenetic-component determination in samples such as fuel, fabric and plastic, uncertainty of ±1 pMC within 30 min of signal averaging is sufficient. While for dating with the bomb-peak curve, ±0.4 pMC means an uncertainty of ±0.4 year for samples in 1980s. For ancient samples 5 kyr ago, in which ¹⁴C radioactivity decayed to half, ±0.4 pMC corresponds to ±62 years in the age determination. The uncertainty achieved in a 2.5-hr measurement guarantees an acceptable precision in the above dating applications. Suess-effect evaluation is probably the most challenge task for current ¹⁴C analytic techniques. As shown in Figure 4, the decreases of ¹⁴C in plants and ambient air are clearly measured by SCAR. However, a continuous measurement to observe the minor fluctuation of ¹⁴C in ambient air has never been realized. The difficulty is the lack of a real-time technique with good enough precision. 0.1 pMC (or even below) is a fair resolution to separate the several-pMC difference between the urban and rural areas. Consequently, the measurement performance of SCAR still needs to be improved.

Finally, in the work for this paper we did not perform δ¹³C measurements. In applications such as Suess-effect evaluation and dating, fractionation correction is required to achieve a fair accuracy. δ¹³C values in the paper are obtained in the following approaches: those of the reference materials are from the supplier; those of the ambient air, the plant leaves, the white wine, the white vinegar and the gelatins are empirical data from literatures (Stuiver and Polach 1977; Troughton and Card 1975); and that of the sediment is from the AMS on-line measurement. Empirical data of δ¹³C contain uncertainties and therefore will enlarge the total uncertainties in deducing pMC or F¹⁴C. In the bio-fraction analysis and medicine applications, we did not perform fractionation corrections. However, an on-line δ¹³C determination procedure can be developed along with SCAR measurement in the future.

Acknowledgments. The authors acknowledge Chinese Academy of Geological Sciences for providing sediment samples and thank Profs. Zhongshan Li, Xiaolei Zhao, Shan Jiang, and Ass. Prof. Hui Zhang for constructive discussions.

Funding statement. This work is supported by “Pioneer” and “Leading Goose” R&D Program of Zhejiang Province, China (Grant Nos. 2022C03084).

Competing interests. The authors declare the following potential conflicts of interest: Luca Varricchio and Amelia Detti are employees, and Saverio Bartalini is the founder of the ppqSense S.r.l.

References

- Aerts-Bijma AT, van der Plicht J and Meijer HAJ (2001) Automatic AMS sample combustion and CO₂ collection. *Radiocarbon* **43**(2A), 293–298. doi: [10.1017/S0033822200038133](https://doi.org/10.1017/S0033822200038133).
- Arjomand A (2010) Accelerator mass spectrometry-enabled studies: Current status and future prospects. *Bioanalysis* **2**(3), 519–541. doi: [10.4155/bio.09.188](https://doi.org/10.4155/bio.09.188).
- Arnold JR and Libby WF (1949) Age determinations by radiocarbon content: checks with samples of known age. *Science* **110**(2869), 678–680. doi: [10.1126/science.110.2869.678](https://doi.org/10.1126/science.110.2869.678).
- Buzynnyi M, Romanenko O, Mykhailova L, et al. (2023) Traces of ¹⁴C emissions for the operation period of two Ukrainian NPPs: Rivne and Chornobyl. *Radiocarbon* **65**(2), 335–342. doi: [10.1017/RDC.2023.3](https://doi.org/10.1017/RDC.2023.3).
- Carcione F, Defeo GA, Galli I, et al. (2023) Material circularity: A novel method for biobased carbon quantification of leather, artificial leather, and trendy alternatives. *Coatings* **13**(5), 892. doi: [10.3390/coatings13050892](https://doi.org/10.3390/coatings13050892).
- Cao Y, Qian Y, Ren H, et al. (2024) Determination of carbon-14 in marine biota using oxidation combustion and gel suspension liquid scintillation counting. *Food Chemistry* **437**, 137914. doi: [10.1016/j.foodchem.2023.137914](https://doi.org/10.1016/j.foodchem.2023.137914).
- Cui X, Newman S, Xu X, et al. (2019) Atmospheric observation-based estimation of fossil fuel CO₂ emissions from regions of central and southern California. *Science of the Total Environment* **664**, 381–391. doi: [10.1016/j.scitotenv.2019.01.081](https://doi.org/10.1016/j.scitotenv.2019.01.081).
- Delli Santi MG, Bartalini S, Cancio P, et al. (2021) Biogenic fraction determination in fuel blends by laser-based ¹⁴CO₂ detection. *Advanced Photonics Research* **2**(3), 2000069. doi: [10.1002/adpr.202000069](https://doi.org/10.1002/adpr.202000069).
- Fahrni SM, Southon JR, Stantos GM, et al. (2017) Reassessment of the ¹³C/¹²C and ¹⁴C/¹²C isotopic fractionation ratio and its impact on high-precision radiocarbon dating. *Geochimica et Cosmochimica Acta* **213**, 330–345. doi: [10.1016/j.gca.2017.05.038](https://doi.org/10.1016/j.gca.2017.05.038).
- Fatima M, Hausmaninger T, Tomberg T, et al. (2021) Radiocarbon dioxide detection using cantilever-enhanced photoacoustic spectroscopy. *Optics Letters* **46**(9), 2083–2086. doi: [10.1364/OL.4201199](https://doi.org/10.1364/OL.4201199).
- Gao L, Li J, Kasserra C, et al. (2011) Precision and accuracy in the quantitative analysis of biological samples by accelerator mass spectrometry: application in microdose absolute bioavailability studies. *Analytical Chemistry* **83**(14), 5607–5616. doi: [10.1021/ac2006284](https://doi.org/10.1021/ac2006284).
- Giusfredi G, Bartalini S, Borri S, et al. (2010) Saturated-absorption cavity ring-down spectroscopy. *Physical Review Letters* **104**(11), 110801. doi: [10.1103/PhysRevLett.104.110801](https://doi.org/10.1103/PhysRevLett.104.110801).
- Galli I, Bartalini S, Ballerini R, et al. (2016) Spectroscopic detection of radiocarbon dioxide at parts-per-quadrillion sensitivity. *Optica* **3**(4), 385–388. doi: [10.1364/OPTICA.3.000385](https://doi.org/10.1364/OPTICA.3.000385).
- Hajdas I (2009) Applications of radiocarbon dating method. *Radiocarbon* **51**(1), 79–90. doi: [10.1017/S0033822200033713](https://doi.org/10.1017/S0033822200033713).
- Hajdas I, Ascough P, Garnett MH, et al. (2021) Radiocarbon dating. *Nature Reviews Methods Primers* **1**(1), 62. doi: [10.1038/s43586-021-00058-7](https://doi.org/10.1038/s43586-021-00058-7).
- Hajdas I, Calcagnile L, Molnár M, et al. (2022) The potential of radiocarbon analysis for the detection of art forgeries. *Forensic Science International* **335**, 111292. doi: [10.1016/j.forsciint.2022.111292](https://doi.org/10.1016/j.forsciint.2022.111292).
- Hogg AG and Cook GT (2022) Liquid scintillation counting (LSC)—past, present, and future. *Radiocarbon* **64**(3), 541–554. doi: [10.1017/RDC.2021.91](https://doi.org/10.1017/RDC.2021.91).
- Hua Q, Turnbull JC, Santos GM, et al. (2022) Atmospheric radiocarbon for the period 1950–2019. *Radiocarbon* **64**(4), 723–745. doi: [10.1017/RDC.2021.95](https://doi.org/10.1017/RDC.2021.95).
- Jiang J and McCart AD (2021) Two-color, intracavity pump–probe, cavity ring-down spectroscopy. *The Journal of Chemical Physics* **155**(10). doi: [10.1063/5.0054792](https://doi.org/10.1063/5.0054792).
- Johnstone-Belford EC, Jacobsen G, Fallon SJ, et al. (2023) The effects of diet and beauty products on the uptake and storage of ¹⁴C in hair and nails: ramifications for the application of bomb pulse dating to forensic anthropological casework. *Forensic Science International* **349**, 111771. doi: [10.1016/j.forsciint.2023.111771](https://doi.org/10.1016/j.forsciint.2023.111771).
- Julien M, Parinet J, Nun P, et al. (2015) Fractionation in position-specific isotope composition during vaporization of environmental pollutants measured with isotope ratio monitoring by ¹³C nuclear magnetic resonance spectrometry. *Environmental Pollution* **205**, 299–306. doi: [10.1016/j.envpol.2015.05.047](https://doi.org/10.1016/j.envpol.2015.05.047).
- Korff SA (1940) On the contribution to the ionization at sea-level produced by the neutrons in the cosmic radiation. *Terrestrial Magnetism and Atmospheric Electricity* **45**(2), 133–134. doi: [10.1029/TE045i002p00133](https://doi.org/10.1029/TE045i002p00133).
- Korff SA and Danforth WE (1939) Neutron measurements with boron-trifluoride counters. *Physical Review* **55**(10), 980. doi: [10.1029/TE045i002p00133](https://doi.org/10.1029/TE045i002p00133).
- Krishnan KA, D'Souza RS, Nayak SR, et al. (2022) Carbon-14 emission from the pressurized heavy water reactor nuclear power plant at Kaiga, India. *Journal of Environmental Radioactivity* **255**, 107006. doi: [10.1016/j.jenvrad.2022.107006](https://doi.org/10.1016/j.jenvrad.2022.107006).
- Kutschera W (2022) The versatile uses of the ¹⁴C bomb peak. *Radiocarbon* **64**(6), 1295–1308. doi: [10.1017/RDC.2022.13](https://doi.org/10.1017/RDC.2022.13).
- Libby WF (1970) Radiocarbon dating. *Philosophical Transactions of the Royal Society of London. Series A, Mathematical and Physical Sciences* **269**(1193), 1–10.
- McCart AD, Ognibene TJ, Bench G, et al. (2016) Quantifying carbon-14 for biology using cavity ring-down spectroscopy. *Analytical Chemistry* **88**(17), 8714–8719. doi: [10.1021/acs.analchem.6b02054](https://doi.org/10.1021/acs.analchem.6b02054).
- Michael B (2012) Using radiocarbon to go beyond good faith in measuring CO₂ emissions. *Science* **337**, 400–401. doi: [10.1126/science.337.6093.400](https://doi.org/10.1126/science.337.6093.400).
- Nazarov EI, Kruzhalov AV, Ekidin AA, et al. (2021) Instruments and methods for measuring ¹⁴C (a review). *Instruments and Experimental Techniques* **64**, 790–795. doi: [10.1134/S0020441221060166](https://doi.org/10.1134/S0020441221060166).

- Palstra SWL and Meijer HAJ (2024) Verification of the age of 10- and 20-year-old Tawny Port wines using radiocarbon. *Food Chemistry* **448**, 139081. doi: [10.1016/j.foodchem.2024.139081](https://doi.org/10.1016/j.foodchem.2024.139081).
- Pataki DE, Randerson JT, Dawson TE, et al. (2010) Understanding movement, pattern, and process on Earth through isotope mapping. In: Springer Netherlands, editors. *Isoscapes*. Springer Netherlands, 407–423. doi: [10.1007/978-90-481-3354-3_19](https://doi.org/10.1007/978-90-481-3354-3_19).
- Quarta G, D'Elia M, Braione E, et al. (2019) Radiocarbon dating of ivory: potentialities and limitations in forensics. *Forensic Science International* **299**, 114–118. doi: [10.1016/j.forsciint.2019.03.042](https://doi.org/10.1016/j.forsciint.2019.03.042).
- Quarta G, Hajdas I, Molnár M, et al. (2022) The IAEA forensics program: results of the AMS ¹⁴C intercomparison exercise on contemporary wines and coffees. *Radiocarbon* **64**(6), 1513–1524. doi: [10.1017/RDC.2022.19](https://doi.org/10.1017/RDC.2022.19).
- Reimer PJ, Thomas AB and Ron WR (2004) Discussion: Reporting and calibration of post-bomb ¹⁴C data. *Radiocarbon* **46**(3), 1299–1304. doi: [10.1017/S0033822200033154](https://doi.org/10.1017/S0033822200033154).
- Stuiver M and Polach HA (1977) Discussion reporting of ¹⁴C data. *Radiocarbon* **19**(3), 355–363. doi: [10.1017/S0033822200003672](https://doi.org/10.1017/S0033822200003672).
- Suess HE (1955) Radiocarbon concentration in modern wood. *Science* **122**(3166), 415–417. doi: [10.1126/science.122.3166.415.b](https://doi.org/10.1126/science.122.3166.415.b).
- Synal HA, Stocker M and Suter M (2007) MICADAS: A new compact radiocarbon AMS system. *Nuclear Instruments and Methods in Physics Research Section B: Beam Interactions with Materials and Atoms* **259**(1), 7–13. doi: [10.1016/j.nimb.2007.01.138](https://doi.org/10.1016/j.nimb.2007.01.138).
- Troughton JH and Card KA (1975) Temperature effects on the carbon-isotope ratio of C₃, C₄ and crassulacean-acid-metabolism (CAM) plants. *Planta* **123**, 185–190. doi: [10.1007/BF00383867](https://doi.org/10.1007/BF00383867).
- Tudyka K and Pawlyta J (2014) Biocomponent determination in vinegars with the help of ¹⁴C measured by liquid scintillation counting. *Food Chemistry* **145**, 614–616. doi: [10.1016/j.foodchem.2013.08.109](https://doi.org/10.1016/j.foodchem.2013.08.109).
- Turnbull JC, Lehman SJ, Miller JB, et al. (2007) A new high precision ¹⁴CO₂ time series for North American continental air. *Journal of Geophysical Research: Atmospheres* **112**(D11), D11310. doi: [10.1029/2006JD008184](https://doi.org/10.1029/2006JD008184).
- Varga T, Hajdas I, Calcagnile L, et al. (2023) Intercomparison exercise on fuel samples for determination of biocarbon ratio by ¹⁴C accelerator mass spectrometry. *Radiocarbon* **65**(2), 539–548. doi: [10.1017/RDC.2023.7](https://doi.org/10.1017/RDC.2023.7).
- Vries HD and Barendsen GW (1953) Radio-carbon dating by a proportional counter filled with carbon dioxide. *Physica* **19**, 987–1003. doi: [10.1016/S0031-8914\(53\)80110-2](https://doi.org/10.1016/S0031-8914(53)80110-2).
- Wang N, Shen CD, Ding P, et al. (2010) Improved application of bomb carbon in teeth for forensic investigation. *Radiocarbon* **52**(2), 706–716. doi: [10.1017/S003382220004720](https://doi.org/10.1017/S003382220004720).
- Wang Y, Luo Z, Tang Y, et al. (2022) Establishment and verification of a metering scheme for biomass-coal blending ratios based on ¹⁴C determination. *Fuel* **327**, 125198. doi: [10.1016/j.fuel.2022.125198](https://doi.org/10.1016/j.fuel.2022.125198).
- Zare RN (2012) Ultrasensitive radiocarbon detection. *Nature* **482**(7385), 312–313. doi: [10.1038/482312a](https://doi.org/10.1038/482312a).
- Zavattaro D, Quarta G, D'Elia M, et al. (2007) Recent documents dating: an approach using radiocarbon techniques. *Forensic Science International* **167**(2–3), 160–162. doi: [10.1016/j.forsciint.2006.06.060](https://doi.org/10.1016/j.forsciint.2006.06.060).
- Zhou W, Niu Z, Wu S, et al. (2022) Recent progress in atmospheric fossil fuel CO₂ trends traced by radiocarbon in China. *Radiocarbon* **64**(4), 793–803. doi: [10.1017/RDC.2022.32](https://doi.org/10.1017/RDC.2022.32).
- Zollinger M, Lozac'h F, Hurh E, et al. (2014) Absorption, distribution, metabolism, and excretion (ADME) of ¹⁴C-sonidegib (LDE225) in healthy volunteers. *Cancer Chemotherapy and Pharmacology* **74**, 63–75. doi: [10.1007/s00280-014-2468-y](https://doi.org/10.1007/s00280-014-2468-y).
- Zoppi U and Arjomand A (2010) Simultaneous AMS determination of ¹⁴C content and total carbon mass in biological samples. *Nuclear Instruments and Methods in Physics Research Section B: Beam Interactions with Materials and Atoms* **268**(7–8), 1307–1308. doi: [10.1016/j.nimb.2009.10.159](https://doi.org/10.1016/j.nimb.2009.10.159).
- Zoppi U, Crye J, Song Q, et al. (2007) Performance evaluation of the new AMS system at Accium BioSciences. *Radiocarbon* **49**(1), 171–180. doi: [10.1017/S00338222000](https://doi.org/10.1017/S00338222000).

Cite this article: Guan Z, Zhou Y, Ling Q, Varricchio L, Detti A, Bartalini S, and Chen D (2025). Laser spectroscopy: A potential versatile solution for radiocarbon analyses. *Radiocarbon* **67**, 565–577. <https://doi.org/10.1017/RDC.2025.10>